ACCELERATED PUBLICATION

This paper is available online at www.jbc.org

⌘ Author's Choice

THE JOURNAL OF BIOLOGICAL CHEMISTRY VOL. 283, NO. 26, pp. 17753–17756, June 27, 2008

Crystal Structure of Squid Rhodopsin with Intracellularly Extended Cytoplasmic Region*[S]

Received for publication, February 5, 2008, and in revised form, April 15, 2008
Published, JBC Papers in Press, May 6, 2008, DOI 10.1074/jbc.C800040200

Tatsuro Shimamura[‡1], Kenji Hiraki[§1], Naoko Takahashi[‡], Tetsuya Hori[‡], Hideo Ago[‡], Katsuyoshi Masuda[§], Koji Takio[‡], Masaji Ishiguro[§2], and Masashi Miyano[‡3]

From the [‡]RIKEN SPring-8 Center, Harima Institute, Kouto, Sayo, Hyogo 679-5148 and the [§]Suntory Institute for Bioorganic Research, 1-1-1 Wakayamadai, Shimamoto-cho, Mishima-gun, Osaka 618-8503, Japan

G-protein-coupled receptors play a key step in cellular signal transduction cascades by transducing various extracellular signals via G-proteins. Rhodopsin is a prototypical G-protein-coupled receptor involved in the retinal visual signaling cascade. We determined the structure of squid rhodopsin at 3.7 Å resolution, which transduces signals through the G_q protein to the phosphoinositol cascade. The structure showed seven transmembrane helices and an amphipathic helix H8 has similar geometry to structures from bovine rhodopsin, coupling to G_t, and human β_2-adrenergic receptor, coupling to G_s. Notably, squid rhodopsin contains a well structured cytoplasmic region involved in the interaction with G-proteins, and this region is flexible or disordered in bovine rhodopsin and human β_2-adrenergic receptor. The transmembrane helices 5 and 6 are longer and extrude into the cytoplasm. The distal C-terminal tail contains a short hydrophilic α-helix CH after the palmitoylated cysteine residues. The residues in the distal C-terminal tail interact with the neighboring residues in the second cytoplasmic loop, the extruded transmembrane helices 5 and 6, and the short helix H8. Additionally, the Tyr-111, Asn-87, and Asn-185 residues are located within hydrogen-bonding distances from the nitrogen atom of the Schiff base.

G-protein-coupled receptors (GPCRs)[4] transduce a diverse class of extracellular signals such as photons, hormones, and glycoproteins to a small number of G-proteins (1, 2). Thousands of GPCRs mediate signals through a limited number of G-protein subtypes, such as G_s, $G_{i/o/t/z}$, or $G_{q/11}$, whose activation in cellular signaling pathways result in up- or down-regulation of cAMP or activation of the phosphoinositol cascade, respectively (2, 3). Several GPCR subtypes recognize the same intrinsic ligand such as adrenaline, histamine, or serotonin, and each subtype transduces the same extracellular stimulus to different G subtypes. Thus, the cytoplasmic portion of each GPCR should have characteristic regions that can discriminate between and activate the correct coupling G-protein. Using software based on hidden Markov models, such as 3D-Coffee and PRED-COUPLE, phylogenetic analyses can distinguish the G-protein specificity of each GPCR, and the G-protein subtype coupled to each GPCR can be classified (3, 4).

Despite intensive structural studies of GPCRs including rhodopsins from diverse organisms, there are only a few available atomic structures of the rhodopsin-type (class A) GPCRs (5–10). Bovine rhodopsin couples to transducin G_t, a pertussis toxin-sensitive G-protein in the $G_{i/o/t/z}$ subtype, and down-regulates cGMP but not cAMP (31). Bovine rhodopsin was previously the only structure-determined GPCR at high resolution in the tetragonal and trigonal crystal forms (5, 6). Recently, the structures of the human β_2-adrenergic receptor (β_2AR) coupling to G_s were determined in a complex with a monoclonal antibody Fab fragment to the third cytoplasmic loop (CL3) and a chimeric form whose entire CL3 region was replaced by T4 lysozyme (7–9).

GPCRs have seven structurally conserved transmembrane helices (TH1–TH7) with various post-translational modifications including N-terminal acetylation, *N*-glycosylation, palmitoylation, and phosphorylation. Both the N-terminal and the C-terminal tails as well as the extracellular and cytoplasmic loop regions (EL1–EL3 and CL1–CL3, respectively) have low sequence homology. Although the extracellular ligand-binding regions are quite distinct, there is the same amphipathic short helix H8 in both bovine rhodopsin and β_2AR (5, 8). The GPCR cytoplasmic region, including the C-terminal tail, should have a structure capable of simultaneously discriminating between G-protein subtypes and activating conserved G-proteins. Some activated GPCRs such as BLT1 can promiscuously activate more than two G subtypes, G_i and G_q (3, 10). Squid rhodopsin couples to bovine G_t as well as the intrinsic G_q (11, 12). Thus, structural information on novel GPCR recognition and coupling to G subtypes would be indispensable for elucidating the recognition and activation mechanisms for each G-protein.

Here, we report the unique crystal structure of G_q coupling rhodopsin from the Japanese flying squid at 3.7 Å resolution in an orthorhombic crystal, as well as confirmation of its chemical structure and post-translational modifications.

EXPERIMENTAL PROCEDURES

Purification of Squid Rhodopsin—All procedures were carried out at room temperature in the dark or under dim red light unless otherwise indicated. Squid rhodopsin was prepared from

* The costs of publication of this article were defrayed in part by the payment of page charges. This article must therefore be hereby marked "*advertisement*" in accordance with 18 U.S.C. Section 1734 solely to indicate this fact.

⌘ *Author's Choice*—Final version full access.

The atomic coordinates and structure factors (code 2ZIY) have been deposited in the Protein Data Bank, Research Collaboratory for Structural Bioinformatics, Rutgers University, New Brunswick, NJ (http://www.rcsb.org/).

[S] The on-line version of this article (available at http://www.jbc.org) contains supplemental text and two supplemental figures.

[1] Both authors contributed equally to this work.

[2] To whom correspondence may be addressed. E-mail: ishiguro@sunbor.or.jp.

[3] To whom correspondence may be addressed. E-mail: miyano@spring8.or.jp.

[4] The abbreviations used are: GPCR, G-protein coupled receptor; PDB, Protein Data Bank; TH, transmembrane helix; CL, cytoplasmic loop; EL, extracellular loop; CH, C-terminal tail helix; NH, N-terminal tail helix; DDM, dodecyl maltoside; β_2AR, β_2-adrenergic receptor; MALDI-TOF, matrix-assisted laser desorption/ionization-time of flight; TOF/TOF, tandem time of flight; MS, mass spectrometry; MS/MS, tandem mass spectrometry.

Todarodes pacificus caught in the Japan Sea, using previously described methods (13). Briefly, the rhabdomeric membranes were isolated from squid retina by repetitive sucrose flotation. The membranes were treated with V8 protease (Pierce, 50:1 w/w of rhodopsin:V8 protease) at room temperature for 1 h to remove the unique C-terminal proline-rich extension of the squid rhodopsin. The reaction was terminated by extensive washing with HEPES buffer (5 mM HEPES, pH 7.0, 1 mM EDTA, 1 mM dithiothreitol). The membranes were solubilized with 2% (w/v) dodecyl maltoside (DDM, Anatrace) for 1 h at 4 °C. After centrifugation, the supernatant was loaded onto a DEAE-cellulose column (Whatman) equilibrated with buffer A (50 mM HEPES, pH 7.0, 0.05% (w/v) DDM). The unbound fraction was collected and applied to a concanavalin A-Sepharose 4B column (Amersham Biosciences) equilibrated with buffer A. The rhodopsin was eluted with 0.2 M α-methyl mannoside solution. Fractions containing squid rhodopsin were pooled and dialyzed against buffer A and then concentrated by ultrafiltration (Amicon Ultra, Millipore).

N-terminal Sequencing and Mass Analyses—The identity and integrity of the purified protein were assessed by N-terminal amino acid sequencing by Edman degradation and various mass spectrometric analyses, including MALDI-TOF/MS, MALDI-TOF/TOF-MS/MS, nano-liquid chromatography-quadrapole TOF-MS/MS, and high performance liquid chromatography-electrospray ionization-iontrap-MS/MS as described in the supplemental materials (14).

Crystallization—Crystals were grown by the hanging-drop vapor diffusion method. One microliter of protein sample (10 mg/ml) in a solution of 10 mM HEPES, pH 7.0, 200 mM NaCl, 2 mM dodecyldimethylamine oxide, 0.03% (w/v) DDM was mixed with 1 μl of reservoir solution (0.1 M HEPES, pH 7.0, 8% (v/v) ethylene glycol, 28% (w/v) polyethylene glycol 400) and left to equilibrate at 20 °C. Crystals appeared after 5 days and stopped growing within 2 weeks.

Structure Determination and Refinement—X-ray diffraction data were collected at 100 K on beam line BL45XU at SPring-8. Data were reduced using the program HKL2000 (15). The structure was determined by molecular replacement with the program MOLREP in the CCP4 program suite (16) using a monomer of the trigonal crystal structure of the bovine rhodopsin (PDB code: 1GZM) (17) as a search model. Refinement and model building were performed iteratively with the programs CNS (18), REFMAC5 in CCP4 (16), and O (19). During refinement, we used grouped, unrestrained *B*-factor refinement with a single group for the entire molecule. All refinements were carried out with 10% of the reflections for cross validation. Despite the low resolution data and the low sequence homology between squid and bovine rhodopsins (24%), the structure was well refined thanks to the structural similarity of the transmembrane helices and the positions for a disulfide bridge, an 11-*cis*-retinal chromophore in the Schiff base linkage, and the conserved residues. *B*-factor sharpening was used to generate detailed maps using the CNS program with B_{sharp} values ranging from -50 to -150 Å^2 (20). Data collection and refinement statistics are shown in Table 1. All figures including electrostatic potential surfaces were prepared using PyMOL (DeLano Scientific LLC). The coordinates have been deposited in the Protein Data Bank (PDB) with the accession code 2ZIY.

TABLE 1
Data collection and refinement statistics

Data collection	
Wavelength (Å)	0.97950
Resolution (Å)	43.2-3.7
Measured reflections	43,571
Unique reflections	6,680
Completeness (%)[a]	93.3 (74.3)
R_{merge} (%)[b]	6.4 (77.5)[c]
Space group	$C222_1$
Unit cell (Å)	$a = 84.3$, $b = 108.7$, $c = 142.2$
Refinement	
Resolution (Å)	43.2-3.7
Reflections used	6,647
R_{work}/R_{free} (%)[d,e]	30.2/33.0 (41.4/43.2)
r.m.s.[f] deviation	
bond (Å)	0.014
angle (°)	2.01
Ramachandran statistics	
Most favored region (%)	70.4
Additional allowed region (%)	27.1
Generously allowed region (%)	2.1
Disallowed region (%)	0.3

[a] Values in parentheses are for the highest-resolution shell (3.83-3.70 Å).
[b] $R_{merge} = \Sigma_i|I(h)_i - \langle I(h)\rangle|/\Sigma_i|I(h)_i|$, where $\langle I(h)\rangle$ is the mean intensity of equivalent reflections.
[c] The last shell R_{merge} is rather high as a result of strong anisotropy.
[d] $R_{work} = \Sigma||Fo| - |Fc||/\Sigma|Fo|$, where *Fo* and *Fc* are the observed and calculated structure factor amplitudes, respectively.
[e] $R_{free} = \Sigma||Fo| - |Fc||/\Sigma|Fo|$, calculated using a test data set, 10% of total data randomly selected from the observed reflections.
[f] r.m.s., root mean square.

RESULTS AND DISCUSSION

Chemical Structure of Squid Rhodopsin—We first confirmed the chemical structure of V8 protease-treated squid rhodopsin. N-terminal sequencing and various MS analyses showed that the squid rhodopsin was cleaved at Glu-373 by the V8 protease, and the polypeptide chain was from Gly-2 to Glu-373 containing a Val to Ile substitution at position 18 with all the expected post-translational modifications. These included *N*-glycosylation and two palmitoylations, as well as a Schiff-based retinal. The molecular mass of squid rhodopsin was 43,842 Da (calculated molecular mass 43,883) by MALDI-TOF MS analysis (supplemental Fig. 1) (14, 21, 22).

Overall Structure—The overall structure of C-terminal truncated squid rhodopsin is a class A GPCR, with seven transmembrane helices, including the amphipathic short helix H8 and a prominent, well ordered cytoplasmic region (see Fig. 2*A*). All amino acid residues except the first 2 residues were defined in the structure, with a disulfide bridge between Cys-108 and Cys-186 in the extracellular region, the 11-*cis*-retinal connected to Lys-305 by the Schiff base, and the two palmitoyl thioesters of Cys-336 and Cys-337. We did not model the *N*-glycan of Asn-8 in the structure due to vague maps, although there were substantial electron densities in $2F_o - F_c$ and $F_o - F_c$ maps where the glycan would be located (supplemental Fig. 2) (22).

Squid rhodopsin has seven transmembrane helices (TH1–TH7) connected by three extracellular (EL1–EL3) and three cytoplasmic (CL1–CL3) loops with N- and C-terminal tails on the extracellular and cytoplasmic sides of the membrane (Fig. 2*A*). The transmembrane helices bend around the conserved proline or glycine residues, especially those with adjacent bulky aromatic residues (Fig. 1) (5, 8). The amphipathic H8 is located just after TH7 at the putative cytoplasmic surface of the mem-

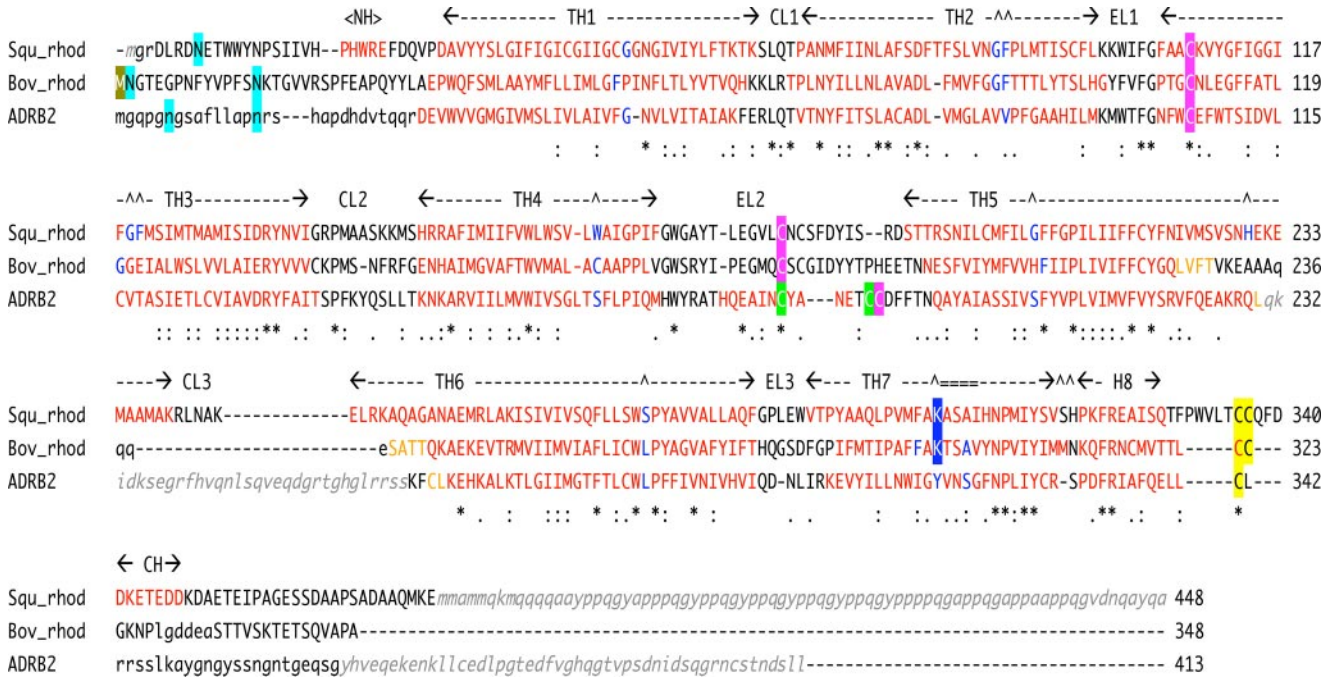

FIGURE 1. **Structural sequence alignment of squid rhodopsin, bovine rhodopsin and β_2AR.** The structural alignment was based on the 3D-Coffee alignment (4). Residues on helix regions are colored *red*, and residue(s) of helix bending are colored in *blue*. Transmembrane helical regions (TH1–TH7) and helix H8 with extracellular (EL1–EL3) and cytoplasmic (CL1–CL3) loops, and each helix in N- and C-terminal tails (NH and CH) are indicated. Posttranslational modifications are shaded by the following colors: *cyan*, *N*-glycosylation; a *pair of pink or green*, disulfide bridge(s); *yellow*, palmitoylated cysteine; *blue*, Schiff-based lysine with 11-*cis*-retinal; *gold*, N-terminal methionine acetylation. Residues indicated by *small letters* are not in models but in crystal protein samples, and residues indicated by *small letters in italic gray* do not exist in the crystal sample proteins due to expression processing, protease digestion, or protein engineering. *Squ_rhod*, squid rhodopsin (PDB code: 2ZIY in this study); *Bov_rhod*, bovine rhodopsin (1F88 (5) or 1GZM (17)); and ADRB2 (2RH1 (8)).

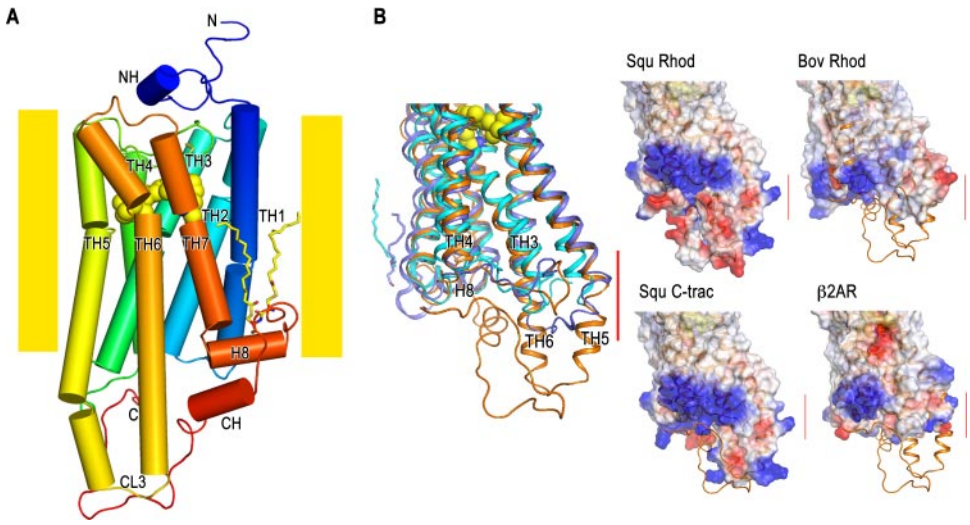

FIGURE 2. **Crystal structure of squid rhodopsin.** *A*, schematic model of squid rhodopsin with multicolored cylindrical helices. Transmembrane helices are indicated as TH1–TH7, and amphipathic short helix H8 is indicated as H8. 11-*cis*-Retinal at Lys-305 and palmitoylated cysteines Cys-336 and Cys-337 are indicated by the *yellow sphere-and-stick models*. A hydrophilic short helix in each N- and C-terminal tail is indicated as NH and CH, respectively. N and C termini are indicated by the letters *N* and *C*, and the cytoplasmic loop 3 is indicated as CL3. Putative transmembrane-spanning regions are indicated by *yellow belts*. *B*, superimposed schematic models and electrostatic surfaces of known GPCR structures. Superimposed schematic structures of squid and bovine rhodopsins, and β_2AR are shown. Squid rhodopsin in this study is shown in *orange*, bovine rhodopsin in the trigonal crystal (1GZM) (17) is *blue*, and β_2AR (2RH1) excluding the T4 lysozyme part of CL3 (8) is *sky blue*. The electrostatic surfaces of squid rhodopsin (*Squ Rhod*), bovine rhodopsin in the trigonal crystal (*Bov Rhod*), and β_2AR (*β2AR*) are represented in *blue* (positive) to *red* (negative) with the squid rhodopsin structure in an *orange schematic*. To clarify the contribution of the distal C-terminal tail, the electrostatic surface of squid rhodopsin without the C-terminal tail after Glu-343 was also calculated (*Squ C-trc*). Different TH5 regions are indicated by the *red line*.

brane and is a conserved structure in rhodopsin-like GPCRs (5, 8, 23). The transmembrane helices of squid rhodopsin can be superimposed on those of bovine rhodopsin and human β_2AR with the root mean square deviations of 1.5 and 2.2 Å, respectively, indicating that the transmembrane helical architecture of the three GPCRs are well conserved, despite many bends in the helices.

The conformation of the N- and C-terminal tails and the CL2, CL3, and EL3 loops differs significantly between bovine and squid rhodopsins, whereas the EL2 conformation is similar to bovine rhodopsin to accommodate the same 11-*cis*-retinal ligand found in visual chromophores. In the proximal C-terminal tail, squid rhodopsin has a 5-residue insertion between H8 and the palmitoylated cysteines, whereas bovine rhodopsin and β_2AR have a palmitoylated cysteine immediately after H8 (Fig. 1) (6, 8).

In the large helix bundle cavity on the extracellular side, 11-*cis*-retinal bonds to Lys-305 with a putative protonated Schiff base, which is countered by the hydroxyl group of Tyr-111 as well as sandwiched by the amides of Asn-87 and Asn-185 at both sides of the retinal within hydrogen bond distances from the Schiff base nitrogen atom (21). The architecture surrounding the Schiff base is consistent with a smaller blue shift upon

photoactivation than that of bovine rhodopsin, whose Schiff base is directly countered by the charged Glu-113 (5, 24).

The extended TH5 and TH6 and the cytoplasmic loops fold into the compact structure (Fig. 2), although squid rhodopsin has longer helices than bovine rhodopsin and β_2AR on the cytoplasmic side (5, 8). Squid rhodopsin has a 12-amino-acid insertion in the CL3 region when compared with bovine rhodopsin (Fig. 1) (21). TH5 elongates to Lys-239 with a bend at His-230 located at the putative cytoplasmic surface of the membrane, in addition to a small bend at Gly-208. TH6 extends from Glu-245 with a bend at Ser-275 before Pro-276 and Tyr-277 (Fig. 2*A*). In the distal C-terminal tail, the residues from Asp-341 to Asp-347 form an additional short hydrophilic C-terminal helix CH. After helix CH, the C-terminal tail from Lys-348 to Glu-373 (which is the C terminus in the V8-treated sample) interacts closely with the extended TH5/TH6 region. The C-terminal region returns to the putative membrane surface in an extended structure via polar interactions with CL2 (Fig. 2). Therefore, the truncated residual polyproline region may align along the surface of the plasma membrane to form the ordered rhabdomeric structure in squid photoreceptor cells (21).

Interaction with G-protein—The cytoplasmic region is folded compactly in squid rhodopsin as described and is thought to interact with the coupling of G_q. The folded region consists of CL2, the helix bundle end of TH5 and TH6 extruded into the cytoplasm as the extended CL3 region, and H8 as well as the distal C-terminal tail including the CH helix. Except for the distal C-terminal tail, these regions interact directly with the respective G-protein in bovine rhodopsin, as shown by peptide competition studies (32). The electrostatic potentials of the cytoplasmic surfaces have a profile characteristic of intracellular GPCR domains (Fig. 2*B*). The distinct electrostatic profiles between these structures are located around the TH5 intracellular surface region of the putative plasma membrane. Interestingly, the corresponding TH5 region was important to G_i coupling but less so to G_q in BLT1 (28). Chemical cross-linking studies of the active form of bovine rhodopsin showed that the CL3 center residues are located close to the G_t-coupled site (29, 30). In the two different crystal forms of bovine rhodopsin, CL3 showed prominent, different conformations (5, 6, 17), whereas the CL3 region was disordered or substituted in both β_2AR structures (7, 8). In the trigonal bovine rhodopsin crystal, CL3 adopts an extended helix-like conformation similar to that of squid rhodopsin (Fig. 2*B*) (17) but not in the tetragonal crystal due to hindrance in the crystal packing by contact with neighboring molecules (5, 6).

The compact hydrophilic intracellular domain of squid rhodopsin on the plasma membrane should participate in recognizing the G-protein during activation. Like other class A GPCRs (26, 27), squid rhodopsin with H8 anchored by the cysteine palmitoylations (Fig. 2*A*) effectively encounters the G-protein anchored by lipid modification(s) on the lateral membrane surface (25). However, the mechanism of G-protein activation by GPCR remains to be further elucidated.

REFERENCES

1. Pierce, K. L., Premont, R. T., and Lefkowitz, R. J. (2002) *Nat. Rev. Mol. Cell Biol.* **3,** 639–650
2. Elefsinioti, A. L., Bagos, P. G., Spyropoulos, I. C., and Hamodrakas, S. J. (2004) *BMC Bioinformatics* **5,** 208
3. Sgourakis, N. G., Bagos, P. G., and Hamodrakas, S. J. (2005) *Bioinformatics* **21,** 4101–4106
4. Poirot, O., Suhre, K., Abergel, C., O'Toole, E., and Notredame, C. (2004) *Nucleic Acids Res.* **32,** W37–40
5. Palczewski, K., Kumasaka, T., Hori., T., Behnke, C. A., Motoshima, H., Fox, B. A., Le Trong, I., Teller, D. C., Okada, T., Stenkamp, R. E., Yamamoto, M., and Miyano, M. (2000) *Science* **289,** 739–745
6. Okada, T., Sugihara, M., Bondar, A. N., Elstner, M., Entel, P., and Buss, V. (2004) *J. Mol. Biol.* **342,** 571–583
7. Rasmussen, S. G., Choi, H. J., Rosenbaum, D. M., Kobilka, T. S., Thian, F. S., Edwards, P. C., Burghammer, M., Ratnala, V. R., Sanishvili, R., Fischetti, R. F., Schertler, G. F., Weis, W. I., and Kobilka, B. K. (2007) *Nature* **450,** 383–387
8. Cherezov, V., Rosenbaum, D. M., Hanson, M. A., Rasmussen, S. G., Thian, F. S., Kobilka, T. S., Choi, H. J., Kuhn, P., Weis, W. I., Kobilka, B. K., and Stevens, R. C. (2007) *Science* **318,** 1258–1265
9. Rosenbaum, D. M., Cherezov, V., Hanson, M. A., Rasmussen, S. G., Thian, F. S., Kobilka, T. S., Choi, H. J., Yao, X. J., Weis, W. I., Stevens, R. C., and Kobilka, B. K. (2007) *Science* **318,** 1266–1273
10. Murakami, M., Kitahara, R., Gotoh, T., and Kouyama, T. (2007) *Acta Crystallogr. F Struct. Biol. Crystalliz. Comm.* **63,** 475–479
11. Sail, H. R., and Michel-Villaz, M. (1984) *Proc. Natl. Acad. Sci. U. S. A.* **81,** 5111–5115
12. Terakita, A., Yamashita, T., Tachibanaki, S., and Shichida, Y. (1998) *FEBS Lett.* **439,** 110–114
13. Kito, Y., Seki, T., and Hagins, F. M. (1982) *Methods Enzymol.* **81,** 44–48
14. Nakamura, T., Dohmae, N., and Takio, K. (2004) *Proteomics* **4,** 2558–2566
15. Otwinowski, Z., and Minor, W. (1997) *Methods Enzymol.* **276,** 307–326
16. Collaborative Computational Project, Number 4. (1994) *Acta Crystallogr. Sect. D Biol. Crystallogr.* **50,** 760–763
17. Li, J., Edwards, P. C., Burghammer, M., Villa, C., and Schertler, G. F. (2003) *J. Mol. Biol.* **343,** 1409–1438
18. Brünger, A. T., Adams, P. D., Clore, G. M., Gros, P., Grosse-Kunstleve, R. W., Jiang, J.-S., Kuszewski, J., Nilges, N., Pannu, N. S., Read, R. J., Rice, L. M., Simonson, T., and Warren, G. L. (1998) *Acta Crystallogr. Sect. D Biol. Crystallogr.* **54,** 905–921
19. Jones, T. A., Zou, J. Y., Cowan, S. W., and Kjeldgaard, M. (1991). *Acta Crystallogr. Sect. A* **47,** 110–119
20. Brünger, A. T. (2007) *Nature Protocols* **2,** 2728–2733
21. Hara-Nishimura, I., Kondo, M., Nishimura, M., Hara, R., and Hara, T. (1993) *FEBS Lett.* **317,** 5–11
22. Takahashi, N., Masuda, K., Hiraki, K., Yoshihara, K., Huang, H. H., Khoo, K. H., and Kato, K. (2003) *Eur. J. Biochem.* **270,** 2627–2632
23. Okuno, T., Yokomizo, T., Hori, T., Miyano, M., and Shimizu, T. (2005) *J. Biol. Chem.* **280,** 32049–32052
24. Terakita, A., Koyanagi, M., Tsukamoto, H., Yamashita, T., Miyata, T., and Shichida, Y. (2004) *Nat. Struct. Mol. Biol.* **11,** 284–289
25. Go, L., and Mitchell, J. (2003) *Comp. Biochem. Physiol.* **B135,** 601–609
26. Delos Santos, N. M., Gardner, L. A., White, S. W., and Bahouth, S. W. (2006) *J. Biol. Chem.* **281,** 12896–12907
27. Okuno, T., Ago, H., Terawaki, K., Miyano, M., Shimizu, T., and Yokomizo, T. (2003) *J. Biol. Chem.* **278,** 41500–41509
28. Kuniyeda, K., Okuno, T., Terawaki, K., Miyano, M., Yokomizo, T., and Shimizu, T. (2007), *J. Biol. Chem.* **282,** 3998–4006
29. Cai, K., Itoh, Y., and Khorana, H. G. (2001) *Proc. Natl. Acad. Sci. U. S. A.*, **98,** 4877–4882
30. Itoh, Y., Cai, K., and Khorana, H. G. (2001) *Proc. Natl. Acad. Sci. U. S. A.* **98,** 4883–4887
31. McLauhlin, S. K., McKinnon, P. J., and Margolskee, R. F. (1992) *Nature* **357,** 563–569
32. König, B., Arendt, A., McDowell, J. H., Kalert, M., Hargrave, P. A., and Hofmann, K. P. (1989) *Proc. Natl. Acad. Sci. U. S. A.* **86,** 6878–6882